Investigation of the Mechanism of Racemization of Litronesib in Aqueous Solution: Unexpected Base-Catalyzed Inversion of a Fully Substituted Carbon Chiral Center

STEVEN W. BAERTSCHI,[1] PATRICK J. JANSEN,[1] ROBERT M. MONTGOMERY,[1] WILLIAM K. SMITH,[1] JERRY R. DRAPER,[1] DAVID P. MYERS,[1] PETER G. HOUGHTON,[1] V. SCOTT SHARP,[1] ANDREA L. GUISBERT,[1] HONG ZHUANG,[1] MICHAEL A. WATKINS,[1] GREGORY A. STEPHENSON,[1] THOMAS M. HARRIS[2]

[1]Eli Lilly and Company, Lilly Research Laboratories, Indianapolis, Indiana 46285-3811
[2]Vanderbilt University, Department of Chemistry, Nashville, Tennessee 37235

Received 8 November 2013; revised 24 January 2014; accepted 10 February 2014

Published online 14 March 2014 in Wiley Online Library (wileyonlinelibrary.com). DOI 10.1002/jps.23918

ABSTRACT: Mitosis inhibitor (*R*)-litronesib (LY2523355) is a 1,3,4-thiadiazoline, bearing phenyl and *N*-(2-ethylamino)ethanesulfonamidomethyl substituents on tetrahedral C5. Chiral instability has been observed at pH 6 and above with the rate of racemization increasing with pH. A positively charged trigonal intermediate is inferred from the fact that a *p*-methoxy substituent on the phenyl accelerated racemization, whereas a *p*-trifluoromethyl substituent had the opposite effect. Racemization is proposed to occur through a relay mechanism involving intramolecular deprotonation of the sulfonamide by the side chain amino group and attack of the sulfonamide anion on C5, cleaving the C5–S bond, to form an aziridine; heterolytic dissociation of the aziridine yields an ylide. This pathway is supported by (1) a crystal structure providing evidence for a hydrogen bond between the sulfonamide NH and the amino group, (2) effects of substituents on the rate of racemization, and (3) computational studies. This racemization mechanism results from neighboring group effects in this densely functionalized molecule. Of particular novelty is the involvement of the side-chain secondary amino group, which overcomes the weak acidity of the sulfonamide by anchimeric assistance. © 2014 Wiley Periodicals, Inc. and the American Pharmacists Association J Pharm Sci 103:2797–2808, 2014

Keywords: racemization; chiral inversion; mechanism; neighboring group; relay ionization; ylide

INTRODUCTION

Chiral integrity is essential to the biological function of many drugs. The maintenance of chiral integrity during manufacture, formulation, storage, and distribution is of paramount importance and is a critical aspect of the development of safe and effective drugs.[1–3] This paper describes an unexpected racemization reaction observed with a novel drug candidate.

In recent years, the molecular motors known as kinesins have emerged as potential targets for cancer chemotherapy. Extensive screening has led to the identification of a number of cell-permeable small molecules that inhibit mitosis by blocking the function of essential spindle proteins other than tubulin. In particular, Eg5 plays a key role in mitosis including chromosome positioning, separating the centrosome, and establishing a bipolar spindle. One such Eg5 inhibitor is the 1,3,4-thiadiazoline (*R*)-litronesib (LY2523355, **1**), which has undergone clinical evaluation for therapeutic treatment of human malignancies.

During the development of a liquid formulation intended for intravenous administration, the observation was made that the chiral purity of (*R*)-litronesib fell during storage of aqueous solutions. Racemization requires the tetrahedral carbon to be transiently converted to a trigonal carbon by rupture of the bond to one of its substituents. The chiral stability of (*R*)-litronesib was excellent under acidic conditions but base-catalyzed racemization was observed at pH values greater than 6. This observation was unexpected because reasonable acid-catalyzed racemization pathways could be proposed, for example, cleavage of the C5–S bond by protonation of N3 to give carbocation (**2**), which would be stabilized by delocalization into the attached nitrogen atom and phenyl ring (Scheme 1). On the contrary, base-catalyzed processes that could be expected to occur even at neutrality were more difficult to envision. As a consequence, a mechanistic investigation was undertaken to elucidate the operative pathway.

EXPERIMENTAL

Materials

Litronesib was obtained from Eli Lilly & Company. Other reagents were obtained from Sigma–Aldrich Chemical Company and used as received.

Nuclear Magnetic Resonance

The nuclear magnetic resonance (NMR) data were acquired on a Varian VNMRS 400 spectrometer equipped with an automated triple band probe. For proton spectra, the typical acquisition parameters included eight scans, a 4.5 s acquisition time, a 45° pulse width, and a 4629.5 Hz sweep width. The FIDs were zero-filled to 32K data points and multiplied by a matched filter exponential window function prior to Fourier transformation.

Abbreviations used: DEA, diethyl amine; DMEA, dimethylethyl amine; IPA, isopropyl alcohol; MP, mobile phase.

Correspondence to: Steven W. Baertschi (Telephone: +317-276-1388; E-mail: baertschi@lilly.com)

This article contains supplementary material available from the authors upon request or via the Internet at http://onlinelibrary.wiley.com/.

Journal of Pharmaceutical Sciences, Vol. 103, 2797–2808 (2014)
© 2014 Wiley Periodicals, Inc. and the American Pharmacists Association

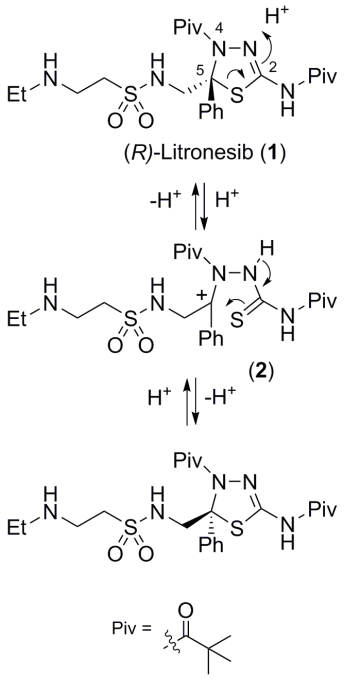

Scheme 1. Postulated acid-catalyzed racemization of (*R*)-litronesib. This pathway was excluded by the effect of pH on the rate of racemization.

The resulting spectra were baseline corrected and referenced to the solvent signal (2.50 ppm). For carbon spectra, the typical acquisition parameters included a 2.6 s acquisition time, a 45° pulse width, and a 25,000 Hz sweep width. The number of scans varied according to the concentration of the sample. The FIDs were zero-filled to 64K data points and multiplied by exponential window function (2 Hz) prior to Fourier transformation. The resulting spectra were baseline corrected and referenced to the solvent signal (39.5 ppm).

Mass Spectrometry

High-resolution positive ion electrospray (ES^+) spectra were obtained by one of the two systems: (1) LC/MS using an Agilent 6230 time-of-flight (TOF) spectrometer coupled to an Agilent 1200 LC system. The system was controlled and data manipulated with Agilent MassHunter software; (2) an LTQ Orbitrap Discovery (ThermoScientific). Nominal mass ES^+ spectra were obtained using a Waters single quadrupole detector mass spectrometer with Waters Empower software.

HPLC Methods

Achiral HPLC analyses were performed on a Waters Acquity UPLC system with photodiode array and electrospray MS detection. The column, a 2.1 × 100 mm BEH-C18, 1.7 μm (Waters), was operated at 45°C. The flow rate was maintained at 0.6 mL/min. Mobile phase (MP) A consisted of 95/5 (v/v) 17 mM acetic acid titrated to pH 5.6 with ammonium hydroxide/acetonitrile, and MP B was acetonitrile. MP B was increased linearly from 0% to 90% at 18% per minute for 5 min and held at 90% for 1 min. Chromatograms were extracted at 240 nm.

Chiral supercritical fluid HPLC analyses were performed on an Agilent 1100 series HPLC modified to pump carbon dioxide and equipped with an Aurora SFC Systems Fusion A5 module. Two different columns were used for the enantiomer analyses; a 4.6 × 150 mm Daicel Chiralpak IA, 5 μm for the *N*-methyl and *N*-acetyl derivatives of litronesib and a 4.6 × 150 mm Daicel Chiracel OD-H, 5 μm for **1**, and the *p*-trifluoromethyl and *p*-methoxy analogs of **1**. The columns were operated at 40°C. The flow rate was maintained at 5.0 mL/min. MP A was liquid carbon dioxide and MP B was methanol containing 0.2% (v/v) triethylamine. MP B was increased linearly from 5% to 15% at 1.25% per minute for 8 min. Chromatograms were extracted at 290 nm.

Preparative Chiral Separations

The preparative chiral separation of the racemic *N*-methyl derivative of litronesib was carried out on an 8 × 35 cm Chiralpak AD column, eluting with 15:85:0.2 ethanol–heptane–DMEA (dimethylethyl amine) (400 mL/min, 290 nm UV detection). The resulting enantiomers were analyzed on a 0.46 × 15 cm Chiralpak AD-H column, eluting with 15:85:0.2 EtOH–heptane–DMEA at 0.6 mL/min (290 nm UV detection).

The racemic *p*-methoxy intermediate (**18a**) was separated on an 8 × 35 cm Chiralpak AD column by eluting with 60/40 heptane–isopropyl alcohol (IPA) (400 mL/min, 310 nm UV detection). The resulting enantiomers were analyzed on a 0.46 × 15 cm Chiralpak AD-H column, eluting with 60/40 heptane–IPA at 0.6 mL/min (280 nm UV detection).

The racemic *p*-trifluoromethyl intermediate (**18b**) was separated by preparative SFC using a Chiralpak AD-H column, with CO_2 and methanol containing 0.1% diethyl amine (DEA) as cosolvent at a wavelength between 214 and 359 nm. The resulting enantiomers were analyzed on a 0.46 × 15 cm Chiralpak AD-H column, eluting with a gradient mixture of MP A: 0.2% DEA in hexane and MP B: 0.2% DEA in EtOH at 0.8 mL/min (5%–15% B after 7 min, held for 8 min, lowered back to 5% B in 1 min and then maintained for a further 9 min, 25 min total run time, 285 nm UV detection).

Ionization Constants

Titrations were performed using Sirius Analytical T3 (T310020) with SiriusT3Control software and SiriusT3Refine Version: 1.1.0.10. Three titrations were performed from pH 2 to 12, in a single vial at varying ratios of cosolvent MeOH–water mixture; conversion to 100% aqueous p*K*a values was accomplished by extrapolation to 0% cosolvent via a Yasuda–Shedlovsky plot. Percentages of cosolvent used for FastpKaUV were approximately 25–34–46; for potentiometric, 30–40–50. Computational p*K*a predictions were made using MarvinSketch™ 5.2.6 (2009) (ChemAxon, Ltd.).

X-Ray Crystallography

A high-quality single crystal of litronesib was grown by recrystallization from 88% acetone and 12% isopropyl ether. The crystal was mounted on a fiber at 100(2) K. Data were collected using a CuKα radiation source (λ = 1.54178 Å) and a Bruker D8 based 3-circle goniometer diffractometer equipped with a SMART 6000CCD area detector (Bruker-AXS, Madison, Wisconsin). Cell refinement and data reduction were performed using the *SAINT* program V7.68a.[4] The unit cell was indexed, having triclinic parameters of $a = 6.2219(3)$ Å, $b = 9.8401(5)$ Å, $c = 11.3183(6)$ Å, and $\alpha = 96.676(3)^\circ$, $\beta = 98.394(3)^\circ$, $\gamma = 103.872(3)^\circ$. The cell volume of crystal structure was 657.23(6) Å^3. The density was calculated to be 1.293 g/cm^3 at 100 K. The

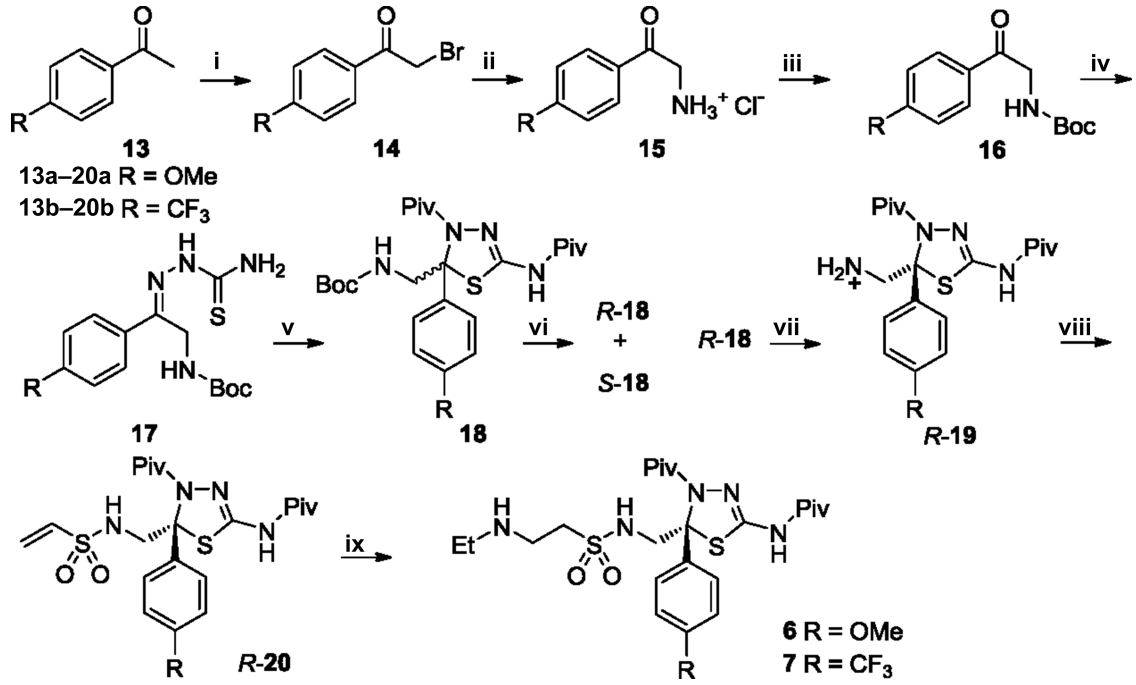

Scheme 2. Preparation of **6** and **7**.[a]

structure was solved by direct methods (*SHELXS86*). All non-hydrogen atomic parameters were independently refined. The space group choice of P1 was confirmed by successful convergence of the full-matrix least-squares refinement on F^2. The final goodness of fit was 1.050. The final residual factor, for all data, was $R1 = 0.0447$ and $wR2 = 0.1078$. The largest difference peak and hole after the final refinement cycle are 0.302 and −0.446 (e A−3), respectively. The absolute stereochemistry (*R* enantiomer) was determined by refinement of the absolute structure parameter to 0.055(18).

Computational Studies

All calculations were performed using the Gaussian 09 Rev B.01 suite of programs[6] with the M062X hybrid functional[7] and the 6–31+G(d) basis set. All geometry optimization and vibration frequency calculations were carried out in a water solvent environment using the self-consistent reaction field model with solvent cavity defined using the polarized continuum model and the universal force field radii model. Internally stored parameters for water were used for solvent calculations. Vibrational frequency analysis was performed to ensure the correct number of negative eigenvalues for each stationary point. Gibbs free energies (ΔG) are used throughout the discussion.

Thiadiazine 4

Litronesib (380 mg) was heated for 3 days at 70°C in 200 mL of 50/50 (v/v) acetonitrile/100 mM $(NH_4)_2HPO_4$. Ultra-performance liquid chromatography analysis of the solution indicated the presence of **4** at a level of 1.8%. A pure sample of **4** (3 mg) was isolated by preparative HPLC. HRMS (ESI-TOF) $m/z = 268.1127$ $(M + H)^+$, $C_{12}H_{18}N_3O_2S^+$, 2.6 ppm error. ^{1}H NMR (500 MHz, DMSO-d_6): δ 8.58 (br s, 3H), 7.58 (d, 2H), 7.50 (m, 3H), 6.52 (br s, 1H), 5.59 (s, 1H), 3.81 (m, 2H), 3.39 (m, 2H), 3.35 (m, 2H), 0.74 (t, 3H). ^{13}C NMR (125 MHz, DMSO-d_6): δ 158.5, 132.7, 129.2, 128.8, 128.5, 48.2, 46.0, 45.7, 42.7, 12.1.

Synthesis of Litronesib Derivatives 6 and 7 (Scheme 2)

The *p*-methoxy derivative (**6**) of (*R*)-litronesib was prepared in nine steps: (1) treatment of 1-(4-methoxyphenyl)ethanone (**13a**) on a 55-g scale with bromine and $AlCl_3$ in MTBE gave bromo-ketone (**14a**) in 78% yield and 91% purity. (2) Amination of **14a** with urotropin and conc. HCl–ethanol in CH_2Cl_2 gave amine hydrochloride **15a** quantitatively; the material was a single peak by HPLC. (3) Protection of amine **15a** with Boc_2O gave Boc-amide **16a** in 67% yield and 96% purity. (4) Reaction of **16a** with thiosemicarbazide afforded thiosemicarbazone **17a** in 84% yield and 99% purity. (5) Cyclization–acylation of **17a** with pivalyl chloride gave racemic thiadiazoline **18a** in 68% isolated yield and 97% purity. MS (ESI) $m/z = 507.6$ $(M + H)^+$, calc: 506.66. ^{1}H NMR (400 MHz, DMSO-d_6) δ 10.85 (s, 1H), 7.17 (d, $J = 8.8$ Hz, 2H), 6.89 (d, $J = 8.8$ Hz, 2H), 6.71 (br s, 1H), 4.34 (dd, $J = 6.7$, 14.48 Hz, 1H), 3.95 (dd, $J = 5.9$, 14.50 Hz, 1H), 3.74 (s, 3H), 1.37 (s, 9H), 1.28 (s, 9H), 1.17 (s, 9H). (6) Preparative HPLC of **18a** (5.2 g) on an 8 × 35 cm Chiralpak AD-H column eluted with 60/40 (v/v) heptane–isopropyl alcohol at 400 mL/min gave the individual enantiomers with ee > 99%. (7) The Boc group was removed from (*R*)-**18a** by treatment of with 5M HCl–EtAc–EtOH at room temperature to give hydrochloride (*R*)-**19a** in quantitative yield and 100% purity. (8 and 9) Treatment of (*R*)-**19a** with $ClCH_2CH_2SO_2Cl$ and Et_3N in 2-MeTHF at −20°C gave sulfonamide (*R*)-**20a** that was treated *in situ* with $EtNH_2$ to give *p*-methoxy derivative (*R*)-**6** of litronesib in 60% yield and 98% purity. The (*S*)-enantiomer was prepared identically. MS (ESI) $m/z = 542.1$ $(M+H)^+$, calc: 541.24. ^{1}H NMR (400 MHz, DMSO-d_6) δ 7.23 (d, $J = 8.7$ Hz, 2H), 6.90 (d, $J = 8.6$ Hz, 2H), 4.28 (d, $J = 13.7$ Hz, 1H), 3.97 (d, $J = 13.8$ Hz, 1H), 3.74 (s, 3H), 3.21 (t, $J = 6.3$ Hz, 2H), 2.88 (t, $J = 6.3$ Hz, 2H), 2.53 (q, $J = 7.1$ Hz, 2H), 1.27 (s, 9H), 1.18 (s, 9H), 0.99 (t, $J = 7.1$ Hz, 3H). ^{13}C NMR (101 MHz, DMSO-d_6) δ 177.4, 174.1, 158.3, 141.1, 134.7, 125.9, 113.7, 82.9, 55.1, 51.5, 46.6, 43.3, 43.0, 26.8, 26.5, 14.9.

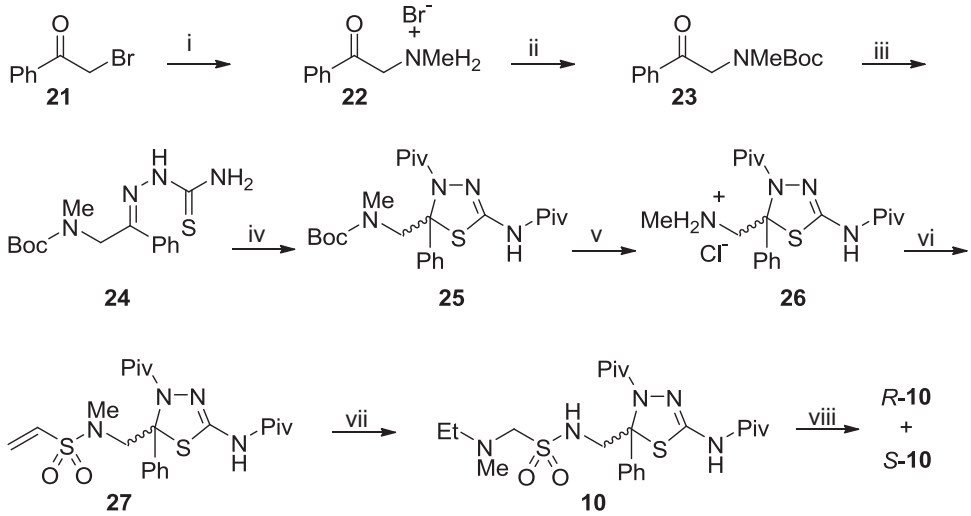

Scheme 3. Preparation of **10**.[a]

The same procedure was used to prepare *p*-trifluoromethyl derivative *(R)*-**7**. (1) Bromo-ketone **14b** was prepared in 59% yield and 95% purity on a 74-g scale. (2 and 3) Amination of **14b** and *in situ* protection gave Boc-protected amine **16b** in 100% crude yield and 58% purity. (4) Without purification, **16b** was converted to thiosemicarbazone **17b** in 86% yield and 94% purity. (5) Cyclization and acylation of **17b** gave thiadiazoline **18b** in 57% isolated yield and 98% purity. MS (ESI) $m/z = 545$ $(M+H)^+$, calc: 544.63. ^{1}H NMR (400 MHz, DMSO-d_6) δ 10.96 (br s, 1H), 7.72 (d, $J = 8.3$ Hz, 2H), 7.48 (d, $J = 8.2$ Hz, 2H), 6.89 (br s, 1H), 4.35 (dd, $J = 6.9$, 14.4 Hz, 1H), 4.00 (dd, $J = 5.9$, 14.41 Hz, 1H), 1.37 (s, 9H), 1.28 (s, 9H), 1.17 (s, 9H). (6) Preparative SFC of **18b** on a Chiralpak AD-H column eluted with CO_2 and MeOH/0.1% DEA gave the individual enantiomers with ee > 99%. (7) The Boc group was removed from *(R)*-**18b** to give hydrochloride *(R)*-**19b** in quantitative yield and 100% purity. (8) Treatment of *(R)*-**19b** with $ClCH_2CH_2SO_2Cl$ gave sulfonamide *(R)*-**20b** that was treated *in situ* with $EtNH_2$ to give *p*-trifluoromethyl derivative *(R)*-**7** of litronesib in 60% overall yield and 98% purity. The *(S)*-enantiomer was prepared identically. MS (ESI) $m/z = 580.1$ $(M+H)^+$, calc: 579.22. ^{1}H NMR (400 MHz, DMSO-d_6) δ 7.73 (d, $J = 8.3$ Hz, 2H), 7.54 (d, $J = 8.3$ Hz, 2H), 4.29 (d, $J = 13.6$ Hz, 1H), 4.03 (d, $J = 13.6$ Hz, 1H), 3.23 (t, $J = 6.3$ Hz, 2H), 2.89 (t, $J = 6.3$ Hz, 2H), 2.53 (q, $J = 7.1$ Hz, 2H), 1.28 (s, 9H), 1.18 (s, 9H), 0.99 (t, $J = 7.1$ Hz, 3H). ^{13}C NMR (101 MHz, DMSO-d_6) δ 177.6, 174.2, 147.2, 125.4, 82.0, 51.5, 46.2, 43.3, 43.0, 26.6, 26.5, 14.9.

Synthesis of *N*-Methyl Derivative 10 (Scheme 3)

The (*R*)-enantiomer of **10** was prepared in eight steps from 2-bromo-1-phenylethanone (**21**): (1) treatment of **21** in acetonitrile with excess methylamine in methanol at low temperature (<0°C) produced amine hydrobromide **22**; (2) direct treatment with $(Boc)_2O$ generated Boc-derivative **23** in 54% overall yield with a purity of 64% (GC-MS). The main impurities were excess $(Boc)_2O$ and BocNHMe, but their presence did not affect the subsequent step. (3) Reaction of **23** with thiosemicarbazide afforded thiosemicarbazone **24** in 40% yield and 97% purity. (4) Cyclization and acylation of **24** with pivaloyl chloride gave racemic Boc-protected thiadiazoline **25** in 78% yield and 95% purity. (5) Deprotection with 5M HCl gave the HCl salt of racemic amine salt **26** in 92% yield and 93% purity. (6 and 7) Acylation of **17** with $ClCH_2CH_2SO_2Cl/Et_3N$/2-Me-THF/−20°C generated the vinyl sulfonamide **27**, which was treated *in situ* with 70% aqueous ethylamine to afford the final racemic **10** in 32% yield and 98% purity after chromatography. MS (ESI) $m/z = 526.2$ $(M+H)^+$, calc: 525.24 ^{1}H NMR (600 MHz, CD_3CN): δ 7.37 (m, 2H), 7.32 (m, 2H), 7.29 (m, 1H), 4.64 (d, $J = 15.2$ Hz, 1H), 4.36 (d, $J = 15.2$ Hz, 1H), 3.25 (m, 2H), 3.00 (m, 2H), 2.94 (s, 3H), 2.62 (q, $J = 7.2$ Hz, 2H), 1.32 (s, 9H), 1.22 (s, 9H), 1.15 (t, $J = 7.2$ Hz). Long-range coupling (HMBC) from the methylene protons at 4.64, and 4.36 ppm to a methyl resonance at 37.0 ppm, and from the methyl protons at 2.62 to the methylene carbon at 52.5 ppm, established the position of a single methyl group on the sulfonamide nitrogen. (8) The enantiomers *(R)*-**10** and *(S)*-**10** were separated by preparative chiral HPLC on an 8 × 35 cm Chiralpak AD column eluted with 15:85:0.2 (v/v/v) ethanol–heptane–DMEA at 400 mL/min and monitored at 290 nm. (*R*)-**10**, MS (ESI) $m/z = 526.2$ $(M+H)^+$, calc: 525.24. ^{1}H NMR (400 MHz, DMSO-d_6) δ 7.37 (t, $J = 7.60$ Hz, 2H), 7.22–7.29 (m, 3H), 4.53 (d, $J = 15.3$ Hz, 1H), 4.32 (d, $J = 15.3$ Hz, 1H), 3.33 (td, $J = 7.2$, 14.0 Hz, 1H), 3.27 (td, $J = 7.0$, 14.0 Hz, 1H), 2.89 (t, $J = 6.9$ Hz, 2H), 2.85 (s, 3H), 2.55 (q, $J = 7.2$ Hz, 2H), 1.30 (s, 9H), 1.18 (s, 10H), 1.00 (t, $J = 7.1$ Hz, 3H). ^{13}C NMR (101 MHz, DMSO-d_6) δ 177.5, 174.8, 142.7, 142.3, 128.6, 127.4, 124.1, 84.5, 51.9, 49.1, 43.0, 42.9, 40.5, 36.6, 26.6, 26.5, 14.9.

(*S*)-**10**, MS (ESI) $m/z = 526.2$ $(M+H)^+$, calc: 525.24. ^{1}H NMR (400 MHz, DMSO-d_6) δ 7.36 (t, $J = 7.6$ Hz, 2H), 7.22–7.30 (m, 3H), 4.53 (d, $J = 15.3$ Hz, 1H), 4.32 (d, $J = 15.4$ Hz, 1H), 3.34 (td, $J = 7.2$, 14.0 Hz, 1H), 3.27 (td, $J = 7.0$, 14.0 Hz, 1H), 2.89 (t, $J = 6.9$ Hz, 2H), 2.85 (s, 3H), 2.55 (q, $J = 7.1$ Hz, 2H), 1.30 (s, 9H), 1.18 (s, 9H), 1.00 (t, $J = 7.1$ Hz, 3H). ^{13}C NMR (101 MHz, DMSO-d_6) δ 177.5, 174.8, 142.7, 142.3, 128.6, 127.4, 124.1, 84.5, 51.9, 49.1, 43.0, 42.9, 40.5, 36.6, 26.6, 26.5, 14.9.

Synthesis *N*-Acetyl Derivative 11

(R)-Litronesib (164 mg) in methylene chloride (15 mL) was treated with 0.5 mL of acetic anhydride (4.9 mmol) for 15 min at ambient temperature. The reaction solution was washed with pH 8 phosphate buffer, dried over anhydrous sodium sulfate, and the solvent evaporated to give **11** as a viscous oil;

purity > 99% by HPLC (220 nm). MS (ESI) m/z = 554.6 $(M+H)^+$, m/z = 552.7 $(M-H)^-$. ^1H NMR (600 MHz, CD_3CN): δ 9.20 (s, 1H), 7.34 (m, 4H), 7.28 (m, 1H), 6.14 (t, J = 7.0 Hz, 1H), 4.50 (dd, J = 7.4, 13.4 Hz, 1H), 3.96 (dd, J = 6.4, 13.4 Hz, 1H), 3.69 (t, J = 6.7 Hz, 2H), 3.34 (q, J = 7.1 Hz, 2H), 3.26 (t, J = 6.7 Hz, 2H), 2.02 (s, 3H), 1.40 (s, 9H), 1.20 (s, 9H), 1.15 (t, J = 7.1 Hz). ^{13}C NMR (151 MHz, CD_3CN): δ 178.5, 176.4, 172.1, 143.6, 142.1, 129.6, 128.7, 125.6, 84.4, 50.6, 48.2, 44.1, 41.3, 40.1, 40.0, 27.1, 27.0, 21.6, 14.1. Long-range coupling (HMBC) from the protons at 3.69, 3.34, and 2.02 ppm to a carbonyl resonance at 171.1 ppm, along with the presence of NH signals at 9.2 and 6.14 ppm, established the location of the acetyl group.

RESULTS AND DISCUSSION

Discovery of Chiral Instability

Stability studies of (*R*)-litronesib were carried out between pH 2.1 and 8.2 at 40°C for up to 93 h using solutions containing 10 mM tartrate adjusted to the reported pH. No degradation could be detected by HPLC analyses using achiral stationary phases, but analyses using chiral stationary phases revealed formation of the (*S*)-enantiomer occurring above pH 6, with progressively increasing chiral instability at higher pH values; additional studies were carried out with similar results in 10 mM sodium chloride, 50 mM phosphate, 10 mM sodium sulfate, and 10 mM methanesulfonic acid (Table 1). A broad pH screen was conducted in 10 mM citrate from pH 2 to 8.4 (Table 2). Together, these data confirmed the chiral instability above pH 6, but no specific buffer or ion effects were detected. Chiral instability was also observed in buffered acetonitrile–water solutions (data not shown).

The effect of temperature was investigated with reaction kinetics being measured at 5°C, 20°C, and 40°C in 10 mM citrate; the pH was adjusted to 8.4 after temperature adjustment and addition of (*R*)-litronesib (Fig. 1). First-order rate constants were calculated using the data from 0% to 40% racemization [i.e., formation of up to 20% of the (*S*)-enantiomer].

Table 1. Chiral Stability of Litronesib at 40°C

Conditions[a]	Time Stressed (h)	S Enantiomer (%)
10 mM tartrate, pH 2.1	96	0.0
10 mM tartrate, pH 3.1	96	0.0
10 mM tartrate, pH 4.1	96	0.0
10 mM tartrate, pH 8.7	124	39.7
50 mM tartrate, pH 2.0	120	0.0
50 mM tartrate, pH 2.9	120	0.0
50 mM tartrate, pH 3.9	120	0.0
50 mM tartrate, pH 6.3	121	1.3
50 mM tartrate, pH 8.4	120	44.8
50 mM tartrate, pH 4.0	97	0.0
10 mM NaCl, pH 8.8	120	42.9
10 mM Na_2SO_4, pH 8.6[b]	120	44.1
10 mM CH_3SO_3H, pH 8.6	96	44.1
50 mM phosphate, pH 2.2	96	0.0
50 mM phosphate, pH 3.3	96	0.0
50 mM phosphate, pH 5.0	96	0.0
50 mM phosphate, pH 6.4	121	1.4
50 mM phosphate, pH 8.3	120	33.8

[a] Litronesib concentration = 0.1 mg/mL.
[b] pH measured before addition of litronesib.

Table 2. Chiral Stability of Litronesib as a Function of pH[a]

Stress Conditions[b]	Time Stressed (h)	S (%)
pH 2.0, 5°C	120	0.0
pH 8.0, 5°C	120	0.7
pH 2.0, RT	120	0.0
pH 3.0, RT	120	0.0
pH 4.0, RT	120	0.0
pH 6.0, RT	120	0.1
pH 8.0, RT	123	20.0
pH 2.1, 40°C	120	0.0
pH 3.3, 40°C	120	0.0
pH 4.2, 40°C	120	0.0
pH 6.2, 40°C	97	1.8
pH 8.4, 40°C	96	40.1

[a] Litronesib concentration = 0.1 mg/mL.
[b] 10 mM citrate; pH measured after addition of litronesib.

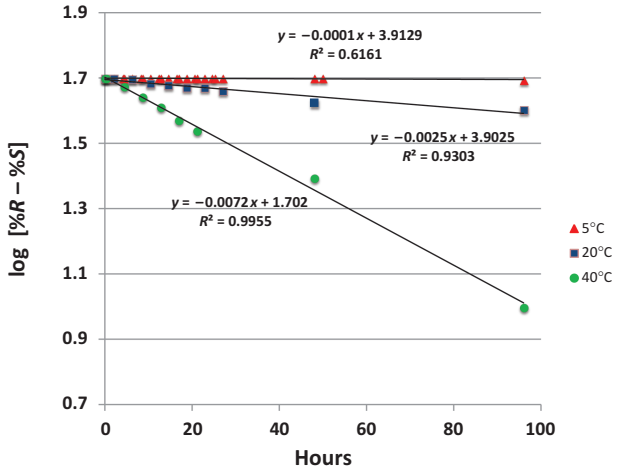

Figure 1. Plot of the log of [%(*R*) enantiomer-%(*S*) enantiomer] of (*R*)-litronesib in pH 8.4 10 mM citrate at 5°C, 20°C, and 40°C over time.

Mechanistic Investigation

Evaluation of Achiral Degradation Pathways

As a first step in the mechanistic investigation, degradation products arising during solution stress testing[8,9] were reviewed to see whether they offered any clue as to the racemization process. HPLC analyses (achiral) of the degradation products resulting from stress tests carried out on litronesib solutions in pH 8 phosphate buffer (0.41 mg/mL, 24 h, 70°C) indicated 11.1% degradation with formation of two major degradation products. The dominant degradation product, ethylenesulfonamide **3**, (9.4% by HPLC-UV peak area) was the result of a simple elimination of ethylamine from the parent molecule. The minor product, thiadiazine **4** (1.1% by HPLC-UV peak area), was of more interest because it arose by a complex process that we viewed as potentially related to the mechanism of racemization. The structures of both compounds were established unequivocally by NMR spectroscopy. The formation of **4** can be rationalized as a β-elimination process in which either the sulfur or the nitrogen attached to C5 is displaced; the proposed

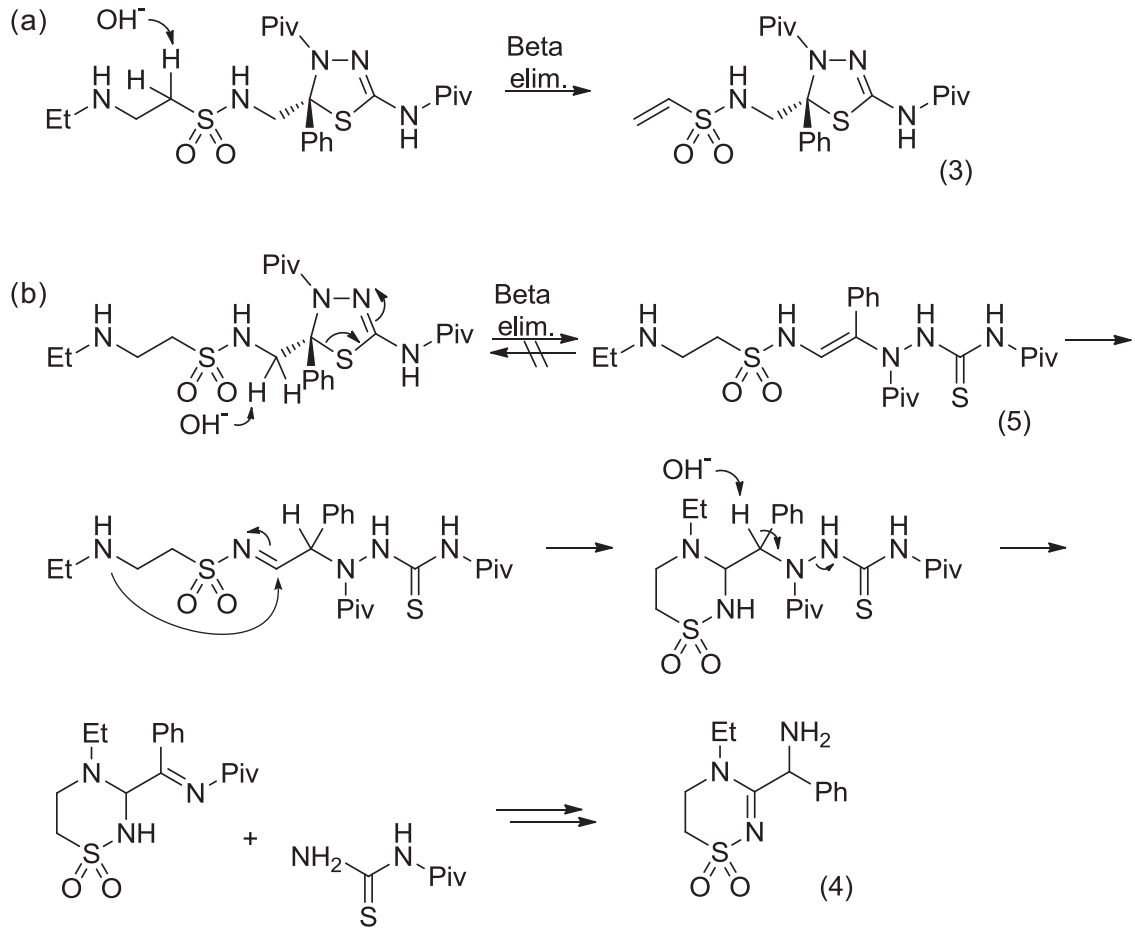

Scheme 4. Achiral degradation pathways involving base-catalyzed β-elimination reactions. Pathway (A) yields degradation product (3). Pathway (B) shows the proposed pathway to degradation product (4). The initial step was shown to be nonreversible by failure to observe deuterium uptake in an H/D exchange experiment, eliminating Pathway B as a possible racemization mechanism.

process involving cleavage of the C5–S bond to give olefin **5** is shown in Scheme 4.

The possibility that racemization might follow a similar course involving formation of trigonal intermediate **5** (or the analogous structure in which the C5–N bond had been broken) followed by reversion to the thiadiazoline was evaluated by incubation of *(R)*-litronesib in CD_3CN:D_2O (95:5, v/v). After 24 h at 55°C, chiral HPLC analysis of the litronesib revealed formation of 14% of the *(S)*-enantiomer (28% racemization), but NMR analysis indicated that deuterium had not been incorporated into the diastereotopic protons of the methylene group of the partially racemized litronesib. On the basis of this result, the β-elimination racemization pathway was rejected.

Possible Formation of an Anion at C5

Consideration was given to the possibility that deprotonation of the pivalamide NH on C2 might initiate base-catalyzed racemization by cleavage of the C5–N bond, which would lead to benzyl anion **5** stabilized by both the phenyl and the divalent sulfur (Scheme 5). To test this proposal, analogs **6** and **7** of litronesib were prepared having electron-donating methoxyl and electron-withdrawing trifluoromethyl substituents, respectively, on the para position of the phenyl ring. The trifluoromethyl substituent can be predicted to increase the rate of racemization by stabilization of the negative charge, whereas the methoxyl substituent would have the opposite effect. The chiral stability of litronesib and the two analogs was evaluated at pH 7.85 in 70/30 phosphate buffer/acetonitrile for 46 h at 40°C (Table 3). This pathway had to be rejected because the results represented by the first-order rate constants shown in Table 3 failed to support the involvement of a benzyl anion; the *p*-trifluoromethyl substituent caused the rate to decrease by approximately a factor of three, whereas the *p*-methoxyl substituent caused a greater than twofold increase.

Formation of a Cation at C5

As a pathway involving anionic species was not supported, consideration was given to pathways involving cationic intermediates. Paths (*a*) and (*b*) in Scheme 6 can be proposed in which racemization would occur via intermediates in which the trigonal benzylic intermediate would bear a positive charge. The processes would be initiated by S_N2 attack of the sulfonamide anion on the fully substituted carbon to form aziridines with inversion of configuration at C5. In Path (*a*), the departing group would be the sulfur moiety to form aziridine **8a**; in Path (*b*), the departing group would be the nitrogen moiety to form aziridine **8b**. In each case, reversible opening of the aziridines to yield a benzyl cation and sulfonamide anion would provide a

 DOI 10.1002/jps.23918

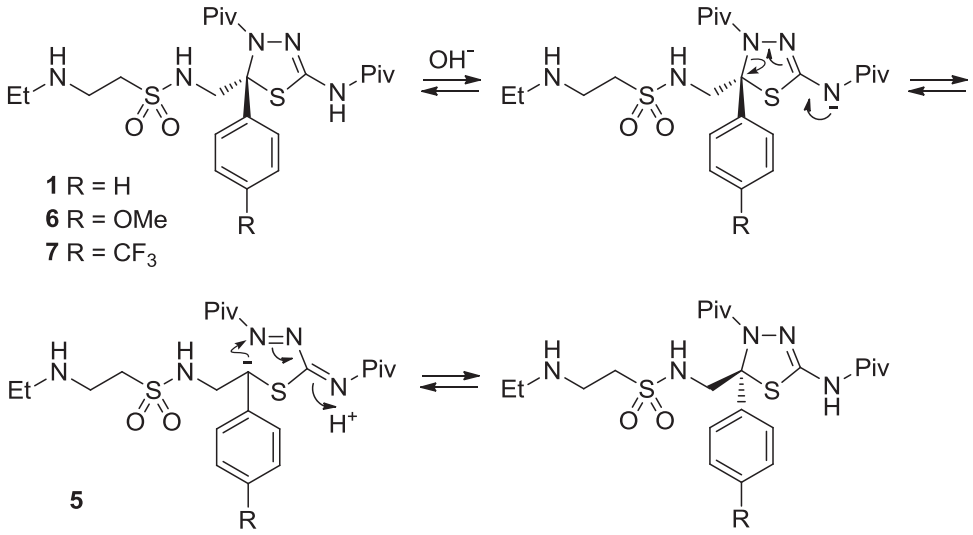

Scheme 5. Postulated base-catalyzed racemization pathway via benzyl anion **5**. This pathway was excluded by the effect of phenyl substituents on the rate of racemization.

Table 3. Racemization of Litronesib and Four Analogs (*S*, %)[a]

Time (h)	Litronesib (1)	*p*-Methoxy (6)	*p*-Trifluoromethyl (7)	*N*-Methyl (10)	*N*-Acetyl (11)
0	0.07	0.96	0.70	0.82	0.03
7	2.36	5.95	1.44	0.89	–
22	6.50	15.37	2.67	0.91	–
26	–	–	–	–	0.04
30	8.64	19.66	3.57	0.85	–
46	12.86	27.34	5.24	0.90	
67	–	–	–	–	0.09
93	–	–	–	–	0.08
k_{obs} (h^{-1})	0.0013	0.0029	0.0004	<0.00001	<0.00001
Relative rate	1.00	2.23	0.31	<0.01	<0.01

[a]Studies were conducted at 40°C in a 70/30 mixture of pH 7.85 buffer and acetonitrile.

pathway for racemization. Literature precedents suggest that the phenyl and tosyl groups alone would not impart sufficient stabilization of the positive and negative charges to promote racemization by this route[10–13]; however, the additional charge compensation in ylides **9a** and **9b** might lower the activation energy sufficiently to promote racemization.

As a test of the validity of these pathways, ionization of the sulfonamide was blocked by methylation. *N*-Methyl derivative **10** (Fig. 2) was prepared as a racemate by a *de novo* synthetic pathway (see *Experimental*), the structure was confirmed by NMR using HMBC correlations to establish the location of the methyl group, and the enantiomers were separated by preparative chiral chromatography. Chiral stability of the (*R*)-enantiomer was evaluated at pH 7.85 (70/30 phosphate buffer/acetonitrile) (Table 3). Less than 0.1% of the (*S*)-enantiomer was detected after 46 h at 40°C, whereas approximately 13% of the (*S*)-enantiomer of litronesib was formed under these conditions. Thus, methylation of the sulfonamide nitrogen effectively shuts down the racemization process, clearly demonstrating direct involvement of the sulfonamide.

Insight as to whether pathway (*a*) or (*b*) (Scheme 6) would be preferred can be gained from consideration of the work of others on thiosemicarbazones, which have been found to be in a dynamic equilibrium with 1,3,4-thiadiazolidines.[14–20] The work of Uda and Kubota[12] is particularly instructive. They observed that under neutral conditions the ring-chain equilibrium between acetone thiosemicarbazone and the corresponding 2-amino-1,3,4-thiadiazoline lies essentially completely on the side of the acyclic species. Likewise, for the thiosemicarbazones formed by condensation of acetone with 1-methyl- and 3-methylthiosemicarbazides, the thiadiazolines are below the level of detection, but the thiosemicarbazone formed with 1,3-dimethylthiosemicarbazide exists totally as the thiadiazoline. Also, they observed that the thiosemicarbazone–thiadiazoline equilibrium is shifted toward the thiadiazoline by acid. Thus, the thiosemicarbazone and 1-methyl- and 3-methylthiosemicarbazones of acetone exist as the thiadiazolines in TFA but revert to the acyclic species on recovery from the acidic solution. Basic conditions favor the acyclic species, although 5,5-dimethyl-2-amino-1,3,4-thiadiazoline remains in the cyclic form in sodium methoxide. We believe litronesib racemization is an extension of these observations and represents the first example of 4-acylthiadiazoline ring-opening occurring without concurrent loss of the acyl group.

The synthetic route to 1,3,4-thiadiazolines provides further insight into the racemization mechanism. Preparatively, thiosemicarbazones of ketones are converted to the thiadiazolines by treatment with acid chlorides or anhydrides; acylation

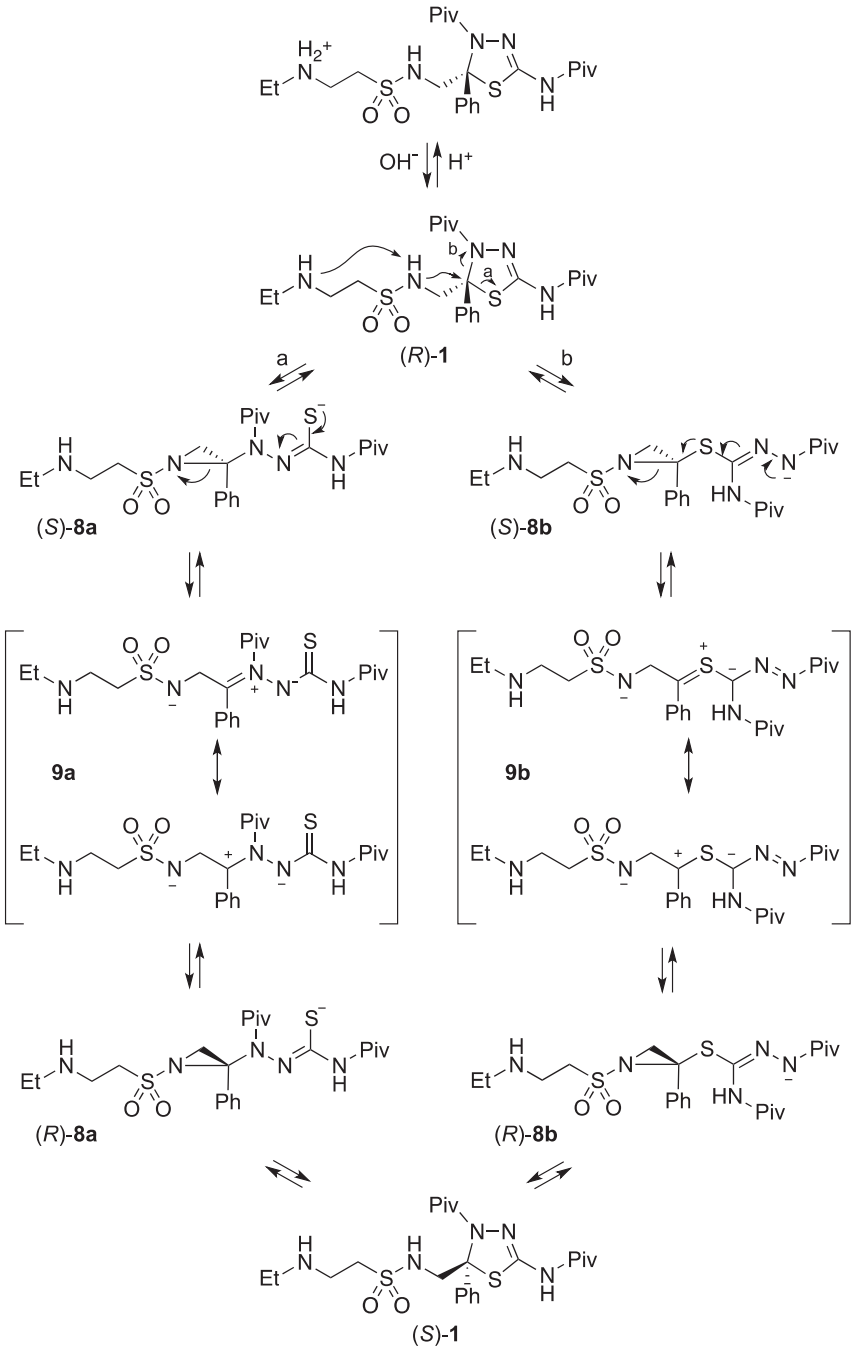

Scheme 6. Proposed relay mechanism for base-catalyzed racemization via an ylide. Both pathways are consistent with all experimental observations, but path (a) is strongly favored by literature precedents and computational studies.

occurs at N4 (and also at the amino group on C2 if it does not already bear substituents).[14,16] The stability of resulting acylated thiadiazolines is dependent on the 4-acyl group remaining in place. Treatment of the N^2,4-diacetyl derivative of 2-amino-5,5-dimethyl-1,3,4-thiadiazoline with 1M NaOH, 1M HCl or even with 10% $NaHCO_3$ causes loss of the acetyl groups and ring opening to yield acetone thiosemicarbazone.[21] These observations about the general route for synthesis of thiadiazolines reinforced by the equilibrium studies of Uda and Kubota[16] lead us to favor the C5-S cleavage over C5-N cleavage [pathway (*a*), Scheme 6).

pKa Measurements (see Fig. 2)

The proposed ylide-mediated racemization pathway is initiated by formation of the sulfonamide anion. Measurements of the p*K*a values of the ionizable functional groups were therefore performed. The UV spectrum of litronesib contains a pH-dependent λ_{max} in the region of 300 nm ($\varepsilon > 10{,}000$), attributed to the thiadiazoline ring system. A p*K*a value of 10.15 for deprotonation of the 2-NH group on the thiadiazoline ring was deduced by curve-fitting analysis from changes in the UV spectrum over the pH range from 8.9 to 11.9.

 DOI 10.1002/jps.23918

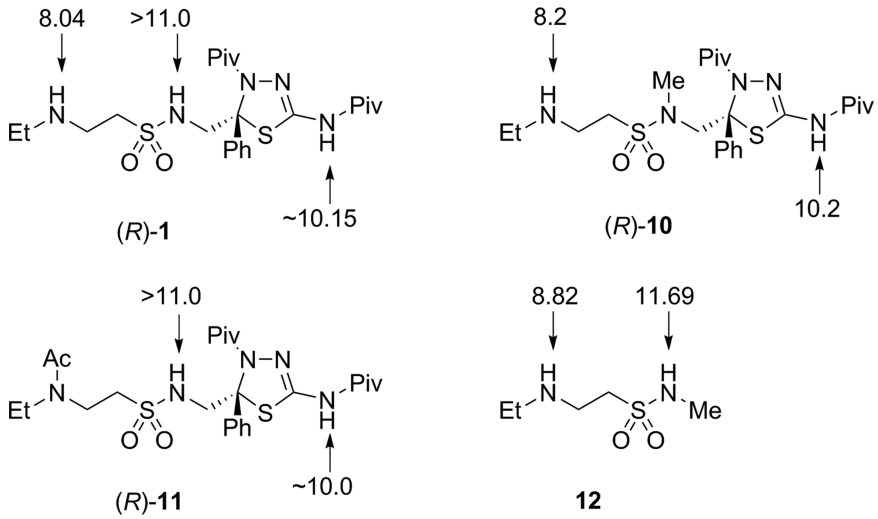

Figure 2. p*K*a values observed for litronesib (**1**) and derivatives **10** and **11**, and values calculated for model sulfonamide **12**.

A potentiometric titration was then carried out to assess the p*K*a values of the UV-silent sulfonamide and the secondary amine. The titration of litronesib (0.197 mmol) with 0.0248M NaOH showed two inflection points. The first was sharp permitting a p*K*a of 8.04 to be deduced by curve fitting; the second inflection was too broad to be analyzed in this manner but was consistent with the p*K*a of 10.15 that has been assigned to the 2-NH by UV titration.

The observed p*K*a of 8.04 can be assigned to deprotonation of the ammonium salt of the secondary amine. The p*K*a of diethylamine is 11.09,[22] but electron withdrawal by the sulfonamide reduces the basicity of the amino group in litronesib. The value of 8.04 is consistent with the p*K*a of the amino group of taurineamide, which has been reported to be 8.08.[23] Junttila and Hormi[24] have reported the p*K*a of methanesulfonamide to be 10.8. The alkyl substituent on the sulfonamide in *N*-acetyl litronesib can be expected to raise the p*K*a of the secondary amine to a value greater than 11. A p*K*a calculation carried out on model compound **12** using the computer program MarvinSketch™ estimated values of 8.82 and 11.69, respectively, for the secondary amino group and sulfonamide NH (see Fig. 2). We conclude that the p*K*a of the sulfonamide group in litronesib is greater than that of the secondary amine group. Thus, the order of ionization events occurring with increasing pH is deprotonation of the secondary ammonium ion followed by the C2 NH and finally the sulfonamide.

Relay Ionization of the Sulfonamide by the Neighboring Secondary Amine

In view of the fact that the first deprotonation event involves conversion of the ammonium ion to the free amine, the potential involvement of the amine in the racemization process was investigated. The approach that was chosen involved acetylation of litronesib to give **11** (Fig. 2), because the *N*-acetyl group would eliminate both the basicity and the nucleophilicity of the amino group. The acetyl group was introduced by direct acetylation with acetic anhydride. The site of acetylation was established by NMR spectroscopy, which showed the expected deshielding of the adjacent methylene protons along with HMBC correlations between the methylene protons and the carbonyl carbon of the acetyl group. UV titration of **11** showed only a p*K*a value of approximately 10.0, which can be assigned to the C2 NH, providing confirmation of the secondary amine assignment for the 8.04 value that had been observed with litronesib. By comparison, compound **10**, having the sulfonamide blocked by methylation, had p*K*a values of 8.2 and 10.2. The chiral stability of **11** was evaluated at pH 7.85 for 93 h at 40°C with the clear cut result that racemization was suppressed more than 100-fold (Table 3). This forces us to conclude that both the sulfonamide and the secondary amine have obligatory roles in the racemization process.

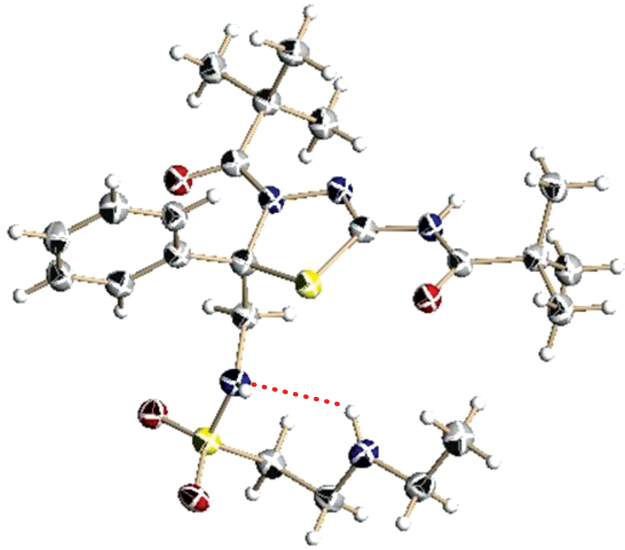

Figure 3. Thermal ellipsoid drawing of the crystal structure of the free base form of (*R*)-litronesib. The sulfonamide and amine nitrogen atoms are 2.99Å apart. The inferred hydrogen bond is indicated with a dashed red line.

Our interpretation of this paradoxical result is that deprotonation of the sulfonamide NH is brought about intramolecularly by proton transfer to the secondary amine rather than by direct reaction with hydroxide ion. An X-ray crystal structure of the free base form of litronesib (Fig. 3) shows that the two nitrogen atoms lie close enough together (2.99 Å) to support a

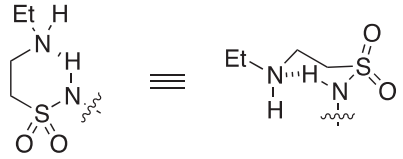

Figure 4. Six-membered ring created by the hydrogen bond between the sulfonamide and the secondary amine.

hydrogen bond between them. Although the X-ray structure did not show proton locations, the orientation of the sulfonamide N–S and N–C bonds permits the sulfonamide proton location to be calculated and placed in juxtaposition with the amino group. The inferred hydrogen bond is shown in Figure 3 as a red dashed line. Figure 4 shows the six-membered ring created by the hydrogen bond. The ring is in a chair conformation with the configurations of the ethyl substituent and thiadiazoline substituents equatorial and axial, respectively.

We conclude the racemization process is being initiated by deprotonation of the secondary ammonium ion. The resulting amine deprotonates the sulfonamide, which in turn attacks C5 to yield aziridine **8a**. The actual racemization process must involve dissociation of the aziridine to form ylide **9a**, although the aziridine was not detected during the course of our investigations of the racemization mechanism.

Computational studies argue for the intermediacy of aziridines and for a carbon–sulfur cleavage in the racemization process as shown in Scheme 6, pathway (*a*). Density functional theory calculations of the potential energy surface carried out at the M062X/6–31+G(d) level of theory for the carbon–sulfur cleavage depicted as pathway (*a*) in Scheme 6 showed well-defined wells for both thiomethine ylide **9a** and the aziridines **8a**. The reaction coordinate is shown in Figure 5. Simultaneous with evaluation of the energetics of the direct and stepwise pathways, a comparison was made between pathways (*a*) and (*b*) in Scheme 6. Potential energy minima were found for aziridines (*S*) and (*R*)-**8b**, although they had significantly higher energies than the aziridines in path (*a*). Collectively, these calculations provide strong support for racemization occurring via aziridines and that pathway (*a*) in Scheme 6 involving aziridines **8a** and ylide **9a** is the likely route. The 16.3 kcal/mol energy barrier difference between the neutral form of litronesib and the aziridine form **8a** coupled with the 5.8 kcal/mol energy barrier between the aziridine form and the zwitterionic species **9a** indicates that the steady-state

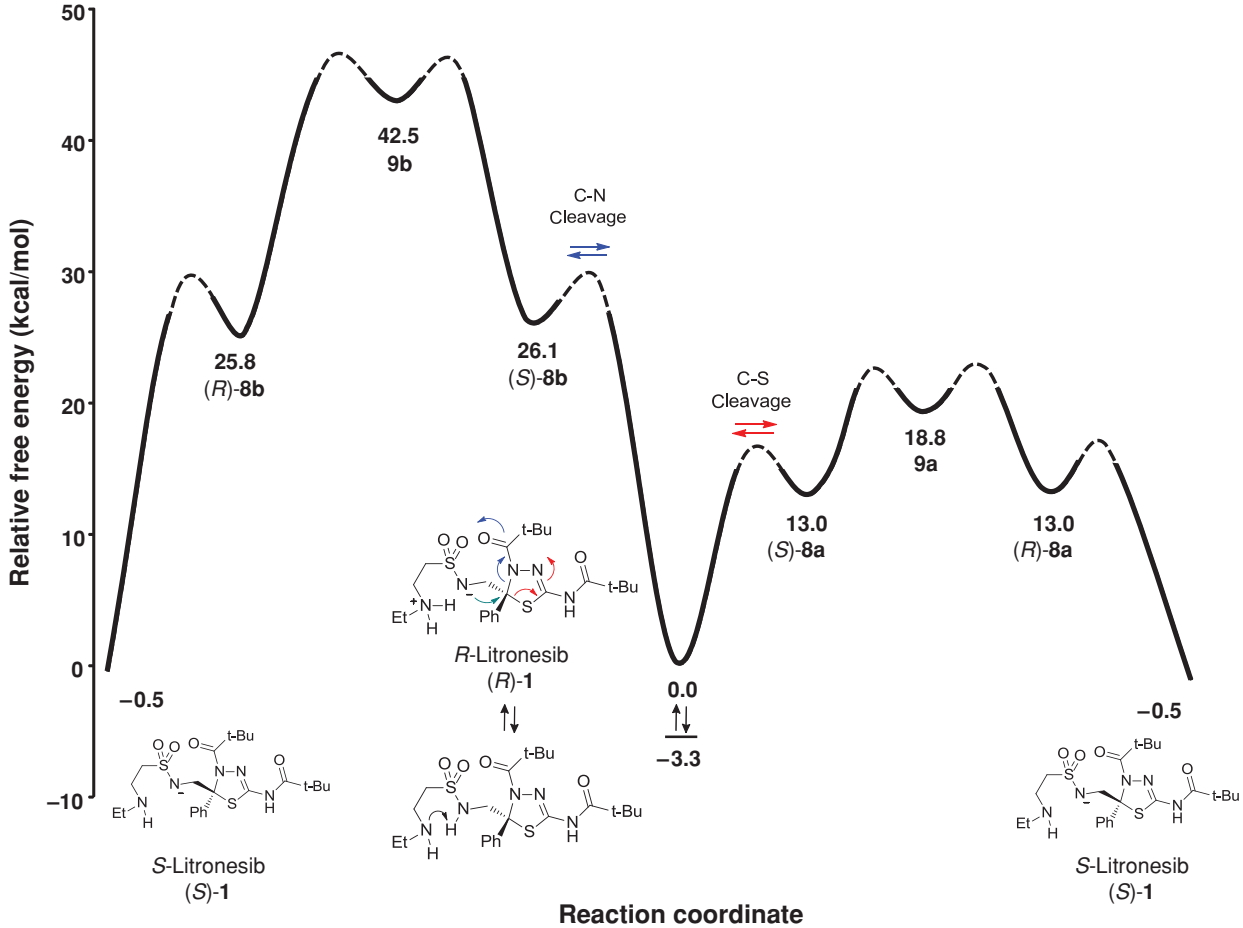

Figure 5. Potential energy surface for the rearrangement of (*R*)-litronesib to (*S*)-litronesib via either a C–S or C–N bond cleavage pathway. Relative free energy of stationary points is normalized to activated (*R*)-litronesib (*R*)-**1**. The activation step (intramolecular deprotonation) is shown to require 3.3 kcal/mol. The computational results indicate the kinetically favored pathway to racemization of (*R*)-litronesib (*R*)-**1** to (*S*)-litronesib (*S*)-**1** is through the C-S cleavage pathway.

 DOI 10.1002/jps.23918

concentrations of the aziridines will be too low to detect by HPLC or the usual spectroscopic tools. Fundamentally, racemization is a slow process, although sufficiently rapid to be a concern when needing to maintain the enantiopurity of a drug during long-term storage in a liquid formulation.

CONCLUSIONS

(*R*)-Litronesib (LY2523355) was discovered to have chiral instability under neutral to basic conditions. An investigation of the mechanism of this instability revealed an unexpected base-catalyzed pathway with neighboring group participation of the secondary amine with the sulfonamide. In support of this pathway, racemization experiments were conducted with four analogs of litronesib. Involvement of charge on the phenyl group was probed with the *p*-methoxyphenyl (electron donating) and *p*-trifluorophenyl (electron withdrawing) analogs. The *p*-methoxy substituent accelerated racemization, whereas the *p*-trifluoromethyl substituent had the opposite effect. These results are consistent with racemization processes involving a thiomethine ylide that places positive charge on the benzylic carbon. Protection of either the sulfonamide nitrogen (as the *N*-methyl derivative) or the secondary amine (as the *N*-acetyl derivative) blocked racemization, indicating their obligatory simultaneous involvement in the racemization process. The preferred side-chain conformation revealed by X-ray crystallography is consistent with a hydrogen bond between the sulfonamide NH and the free base form of the amine. A relay ionization process is postulated in which the free base form of the amine abstracts the sulfonamide proton and the resulting sulfonamide anion attacks C5 with expulsion of the sulfur moiety to form an aziridine. Racemization is proposed to occur by a reversible dissociation of the aziridine to form a thiomethine ylide, which derives stabilization from the partial negative charge on the hydrogen-bonded sulfonamide. Racemization might have involved cleavage of either the C5–S or the C5–N bond, but computational studies and literature precedents provide strong support for cleavage of the bond to sulfur.

The racemization mechanism for litronesib is unique. Although at the outset we expected racemization to involve acid catalysis (see Scheme 1), the experimental results revealed that the process was in fact base catalyzed. This extraordinary mechanism results from neighboring group effects in this densely functionalized molecule. Of particular novelty is the involvement of the side-chain amino group in a relay ionization process that overcomes the weak acidity of the sulfonamide.

ACKNOWLEDGMENTS

The authors gratefully acknowledge Peter Wipf (University of Pittsburgh), Nicholas A. Magnus (Lilly), and Marvin Hansen (Lilly) for helpful discussions. We are grateful to the following people for important contributions to this research: Benjamin A. Diseroad (Lilly) contributions to determining the X-ray single-crystal structure of **1**; Jaclyn Barrett (Lilly) for determining the ionization constants; Jonas Buser and Tim A. Smitka for NMR characterization of **4**, **10**, and **11**; Scott A Bradley and Shanna Neely for NMR characterization of **6**, **7**, and **18**; Thomas M. Zennie for performing the deuterium exchange NMR experiment; Yang Liu and Xianbo Wang (PharmExplorer, Shanghai, China) for the synthesis of **6** and **7**; Gejian Yang (PharmExplorer) for synthesis of racemic **10**; Eric Seest (Lilly) for separation of the enantiomers; Jinxing Ye, Feng Yu, Haoxiang Hu, and Junzhu Lu (East China University of Science and Technology, Shanghai, China) for synthesis of racemic **17**; and Matt Belvo (Lilly) for separation of the enantiomers.

The authors declare no competing financial interest.

REFERENCES

1. Wozniak TJ, Bopp RJ, Jensen EC. 1991. Chiral drugs: An industrial analytical perspective. J Pharm Biomed Anal 9:363–382.
2. De Camp WH. 1993. Chiral drugs: The FDA perspective on manufacturing and control. J Pharm Biomed Anal 11:1167–1172.
3. Lin G-Q, Zhang J-G, Cheng J-F. 2011. Overview of chirality and chiral drugs. Chiral drugs. Hoboken, New Jersey: John Wiley & Sons. Chapter 1, pp 3–28.
4. Sheldrick GM. 1990. Phase annealing in SHELX90: Direct methods for larger structures. Acta Cryst A46:467–473.
5. Sheldrick GM. 1993. SHELXS93. Program for crystal structure refinement. Göttingen, Germany: Institute fur anorganische Chemie.
6. Frisch MJ, Trucks, GW, Schlegel HB, Scuseria GE, Robb MA, Cheeseman JR, Scalmani G, Barone V, Mennucci B, Petersson GA, Nakatsuji H, Caricato M, Li X, Hratchian HP, Izmaylov AF, Bloino J, Zheng G, Sonnenberg JL, Hada M, Ehara M, Toyota K, Fukuda R, Hasegawa J, Ishida M, Nakajima T, Honda Y, Kitao O, Nakai H, Vreven T, Montgomery Jr JA, Peralta JE, Ogliaro F, Bearpark M, Heyd JJ, Brothers E, Kudin KN, Staroverov VN, Kobayashi R, Normand J, Raghavachari K, Rendell A, Burant JC, Iyengar SS, Tomasi J, Cossi M, Rega N, Millam JM, Klene M, Knox JE, Cross JB, Bakken V, Adamo C, Jaramillo J, Gomperts R, Stratmann RE, Yazyev O, Austin AJ, Cammi R, Pomelli C, Ochterski JW, Martin RL, Morokuma K, Zakrzewski VG, Voth GA, Salvador P, Dannenberg JJ, Dapprich S, Daniels AD, Farkas Ö, Foresman JB, Ortiz JV, Cioslowski J, Fox DJ. 2009. Gaussian 09, Revision B.01. Wallingford, Connecticut: Gaussian, Inc.
7. Zhao Y, Truhlar DG. 2008. The M06 suite of density functionals for main group thermochemistry, thermochemical kinetics, noncovalent interactions, excited states, and transition elements: Two new functionals and systematic testing of four M06-class functionals and 12 other functionals. Theor Chem Account 120:215–241.
8. International Conference on Harmonisation Q1A(R2). 2003. Guidance for industry: Stability testing of new drug substances and products, (Second Revision).
9. 2011. Pharmaceutical stress testing: Predicting drug degradation. In Drugs and the pharmaceutical sciences; Baertschi SW, Reed RA, Alsante KM, Eds. Vol. 210. London, UK: Informa Healthcare.
10. Tseng CC, Terashima S, Yamada S-I. 1977. Stereochemical studies. XLV. A novel regiospecific ring opening of optically active 2-substituted-1-tosylaziridines. Chem Pharm Bull 25:166–177.
11. Davis FA, Zhou P, Liang C-H, Reddy RE. 1995. Addition of dimethyloxosulfonium methylide to enentiomerically pure sulfinimines: Asymmetric synthesis of 2-substituted aziridines. Tetrahedron Asymmetry 6:1511–1514.
12. Ghorai MK, Das K, Kumar A, Ghosh K. 2005. An efficient route to regioselective opening of *N*-tosylaziridines with zinc(II) halides. Tetrahedron Lett 46:4103–4106.
13. Colpaert F, Mangelinckx S, De Brabandere S, De Kimpe N. 2011. Asymmetric synthesis of α-chloro-β-amino-*N*-sulfinyl imidates as chiral building blocks. J Org Chem 76:2204–2213.
14. Karabatsos GJ, Vane FM, Taller RA, Hsi N. 1964. Structural studies by nuclear magnetic resonance. VIII. Ring-substituted phenylhydrazones, semicarbazones, and thiosemicarbazones. J Am Chem Soc 86:3351–3357.
15. Mayer KH, Lauerer D, Ring/Ketten-Tautomerie bei. 1970. 1.3.4-Thiadiazolidine-thionen-(2) und Δ^2–1,3,4-thiadiazolinen. Liebigs Ann Chem 731:142–151.

16. Uda M, Kubota S. 1979. Ring-chain tautomerism of acetone *N*-methylated thiosemicarbazones. J Heterocyclic Chem 16:1273–1275.
17. Kubota S, Toyooka K, Ikeda J, Yamamoto N, Shibuya M. 1983. Synthesis of 5-(substituted phenyl) 4-acetyl-2-methylthio-Δ^2–1,3,4-thiadiazolines and their oxidation with potassium permanganate. J Chem Soc Perkin Trans I: 967–1971.
18. Tao EVP, Staten GS. 1984. Synthesis of some *N*-(4,5,5-trisubstituted-Δ^2–1,3,4-thiadiazolin-2-yl)-*N*,*N*′-dimethylureas. Heterocyclic Chem 21:599–601.
19. Toyooka K, Takeuchi Y, Taira Z, Kubota S. 1989. Synthesis of novel chiral 2,3-dihydro-1,3,4-thiadiazoles with extremely high rotations: X-ray crystal structure of (2*R*)-D-mandelyl-5-methylthio-2-phenyl-2,3-dihydro-1,3,4-thiadiazole. Heterocycles 29:1233–1236.
20. Murakata C, Kato K, Ohta Y, Nakai R, Yamashita Y, Takahashi T. 2008. Thiadiazoline derivative. Patent US7425636B2.
21. Kubota S, Ueda Y, Fujikane K, Toyooka K, Shibuya M. 1980. Synthesis of 4-acyl-2-(acylamino)-Δ^2–1,3,4-thiadiazolines and 4-acyl-2-amino-Δ^2–1,3,4-thiadiazolines by acylation of thiosemicarbazones. J Org Chem 45:1473–1477.
22. Perrin DD. 1965. Dissociation constants of organic bases in aqueous solution. IUPAC Chem. Data Ser. London, UK: Butterworths.
23. Kirsch LE, Sihn Y-S. 1997. The effect of polyvinylpyrrolidine on the stability of taurolidine. Pharm Dev Technol 2:345–356.
24. Junttila MH, Hormi OO. 2009. Methanesulfonamide: A cosolvent and general acid catalyst in Sharpless asymmetric dihydroxylations. J Org Chem 7:3038–3047.